Maden Tetkik ve Arama Dergisi

http://dergi.mta.gov.tr

# Mineralogy and geochemistry of kaolinitic clays in the Şile Neogene Basin (İstanbul, Türkiye)

Bala EKİNCİ ŞANS[a*], Oral SARIKAYA[a], Fahri ESENLİ[a], Şenel ÖZDAMAR[a], Hakan TUNÇDEMİR[b], Ümit KARADOĞAN[c], Mustafa KUMRAL[a]

[a] İstanbul Technical University, Department of Geological Engineering, Maslak, 34469, İstanbul, Türkiye

[b] İstanbul Technical University, Department of Mining Engineering, Maslak, 34469, İstanbul, Türkiye

[c] İstanbul Technical University, Department of Civil Engineering, Maslak, 34469, İstanbul, Türkiye

*Research Article*

Keywords:
Clay mineralogy,
Geology, Kaolinite,
Neogene, Şile.

**ABSTRACT**

Şile Neogene Basin (ŞNB) is one of the world's crucial sedimentary clay-sand-coal basins, where approximately 3 million tons of clay and 20 million tons of sand are produced annually. The ŞNB, with a thickness of <54 m, lies unconformably on partly Paleozoic and partly Mesozoic basement units. Clay levels with a total thickness of <21 m comprise mainly kaolinite, quartz and illite, and small amounts of Ca-smectite, mixed-layered phase (I/S), feldspar, siderite, chlorite, muscovite (+/- sericite), anatase, iron oxides/hydroxides, alunite and pyrite. Geochemically, most of the major oxides and SiO2/Al2O3 ratios do not show significant changes on the vertical or lateral scale. On the other hand, K2O, trace elements, REE contents and Th/U ratios of the clay levels overlaying the Paleozoic sandstones are higher than the clays overlaying the Mesozoic volcanics. REEs are higher in the lower part of the Neogene sequence than in the upper part. The mineralogical and geochemical data show that the existing material of ŞNB is an accumulation of different basement rock groups, the mineral type and size of the transported fragments varied at short intervals and carried the effects of various environmental conditions and alteration types.

*Received Date: 25.12.2024*
*Accepted Date: 22.01.2025*

## 1. Introduction

Clayification, in general, and kaolinitization, in particular have essential clues in interpreting sedimentary basins. Kaolin and kaolinitic clays are the type-lithology of the near-surface continental environments (Dill, 2016). One of the types of kaolinization is secondary/sedimentary kaolin formation, as transported and deposited levels within the sedimentary rocks (Prasad et al., 1991; Murray and Keller, 1993; Dill, 2016). Primary kaolinization in residual weathering or hydrothermal alteration is common worldwide. In contrast, sedimentary kaolinite formation is rare due to the deposition and preservation of secondary kaolin deposits requiring special geological conditions (Murray and Keller, 1993). Some kaolin deposits commonly occur in swamp environments rich in organic matter (Spears and Kanaris-Sotiriou, 1979; Zhou et al., 1982; Senkayi et al., 1984). On the other hand, kaolinite is much more common than other members of the group (dickite, nacrite, and halloysite) because it can form at low temperatures lower than 150 °C in sedimentary rocks (Zotov et al., 1998). Kaolinite in sedimentary sequences is generally of authigenic origin (Huggett, 2005).

Economically mineable numerous kaolin deposits formed as hydrothermal and weathering types have been reported from Türkiye (Ömeroğlu Sayıt et al., 2018; Yanık et al., 2018; Çiflikli, 2020; Laçin et al., 2021; Çelik Karakaya et al., 2021; Ünal Ercan et al., 2022; Kadir et al., 2022 and references therein). However, Şile kaolinitic clay deposit, also known as Şile ceramic clay, is the only sedimentary deposit in Türkiye and has been a significant very important industrial raw materials production place for over a century. Within the framework of clay formations in the Istanbul Tertiary Units, Şile and Ağaçlı (İstanbul)

Citation Info: Ekinci Şans, B., Sarıkaya, O., Esenli, F., Özdamar, Ş., Tunçdemir, H., Karadoğan, Ü., Kumral, M. 2025.Mineralogy and geochemistry of kaolinitic clays in the Şile Neogene Basin (İstanbul, Türkiye). Bulletin of the Mineral Research and Exploration xxx, x-x. https://doi.org/10.19111/bulletinofmre.1627560

*Corresponding author: Bala EKİNCİ ŞANS, bekinci@itu.edu.tr

clays have special importance (Esenli and Ekinci Şans, 2023). The ŞNB is located on the Black Sea coast in the north of İstanbul (NW Türkiye) and consists of industrial clay levels (kaolinitic clays), thin coal seams (lignite) and industrial sand levels (quartz-rich). These clay-coal-sand levels are associated with the Oligo-Miocene sedimentary sequence deposited in stream, lake and swamp environments. Some researchers have reported the clay reserves between 53-250 million tons and sand reserves between 100-560 million tons in the basin (Erdoğan et al., 2023; Esenli et al., 2024 and references therein). More than 3 million tons of clay and 20 million tons of sand are produced annually from the quarries of fifteen companies in the basin. The clay raw material of the ŞNB supports the ceramic and refractory industry of Türkiye and various European countries. On the other hand, the sand material in ŞNB is used in construction, casting, ceramics, and chemical industries. Essentially, levels of the basin other than those rich in kaolinite or quartz sand are also important. For example, the presence of kaolinite, illite, quartz and feldspar minerals in different percentages in kaolin deposits may be suitable for different usage areas (Omang et al., 2019). In recent years, special uses of kaolinite-based products have become widespread (Cao et al., 2020; Gianni et al., 2021).

Geological setting, mineralogy, geochemistry and genesis of the sedimentary kaolin deposits in the Şile region have been described by some researchers (Ercan, 1979; Yeniyol, 1984; Yeniyol and Ercan, 1989; Özdamar, 1998; Çoban et al., 2002; Ece et al., 2003; Özdamar et al., 2007; Esenli et al., 2024). Yeniyol (1984) explained the sedimentary kaolin formation of the ŞNB, and Çoban et al. (2002) and Özdamar et al. (2007) studied the mineralogy of underclay in some locations of the region. Esenli et al. (2024) reported general mineralogical and chemical summaries of the sand and clay in the basin. The occurrence, mineralogy and major oxides geochemistry of kaolin deposits, which are representative of some area of the basin, were discussed by Ece et al. (2003) and Ece and Nakagawa (2003). According to Yeniyol (1984) there are two types of kaolinization in the Şile Region. The first was formed in situ by weathering alteration of Upper Cretaceous volcanics (mostly andesite), which are currently buried under Miocene sediments. The second, sedimentary kaolin deposits, were formed due to post-depositional alteration by humic and fulvic acids (Ece et al., 2003). Yeniyol and Ercan (1989) reported that intercalated levels of kaolinitic clay-coal-sand formed during Oligocene-Miocene in swamp and lake environments in response to cyclic paleoclimatic conditions and variable regional tectonic uplift rates.

The researchers mentioned above significantly contributed to our understanding of the environmental conditions of ceramic clays in the ŞNB. Nevertheless, both its formation and the Paleozoic-Mesozoic relationship are still controversial. This paper is a comprehensive study to compare and interpret the horizontal and vertical modal-mineralogically and geochemically (major oxides, trace and rare earth elements) of samples from seven vertical sections (i.e. seven open pits), representing a large part of the basin. In addition to the general interpration of the basin, the paper aims to reveal the mineralogical and geochemical differences of clay levels overlaying Paleozoic sediments and Mesozoic volcanic rocks.

## 2. Geological Setting

East Istanbul, which includes the Şile region, is tectonically located within the Istanbul Zone between Strandja Zone in the west and Sakarya Zone in the east (Okay et al., 1994; Yılmaz et al., 1997; Okay and Kylander-Clark, 2023) (Figure 1). The points of the vertical sections (S1 to S7) sampled in this study are shown on geological map of the region (Figure 1). In the region, the pre-Tertiary basement consists of Paleozoic and Mesozoic-aged units. Paleozoic-aged non-metamorphic sedimentary units are mostly Ordovician quartzite, Silurian conglomerate- arkose-limestone, and Devonian-Carboniferous shale-greywacke-limestone. This group also includes trachy-andesite dykes. Mesozoic (Triassic and Upper Cretaceous) aged units are siliceous sedimentaries, granodiorite and volcanic units (Abdüsselamoğlu, 1963; Baykal and Kaya, 1965; Kaya, 1973; Akyüz, 2010; Özgül, 2011; MTA, 2017; Ayanoğlu, 2018). These basement rocks are unconformable overlain by Tertiary sedimentary successions deposited in a continental margin basin (Tüysüz, 1999). The Tertiary group consists of Eocene (or Paleocene-Eocene) aged limestones, marls, conglomerates and sandstone, and Neogene aged clay, coal and unconsolidated sand (+gravel) (Baykal, 1943; Baykal and Önalan, 1979; Gedik et al., 2005; Özgül, 2011; Özşahin ve Ekinci, 2013; MTA, 2017) (Figure 1). Upper Cretaceous volcanics are silicified and kaolinized andesite, quartz andesite, dacite-type lavas, and pyroclastics (Yeniyol and Ercan, 1989; Keskin et al., 2003). These volcanics are the products of Turonian volcanic activity that developed due to the first arc magmatism related to the north subduction of the Neotethys Ocean during the Late Cretaceous-Early Tertiary period (Baykal, 1943; Şengör and Yılmaz, 1981; Tüysüz, 1999).

Neogene sequence overlaid the Mesozoic volcanic rocks (mainly andesites) in some areas of the Şile region and the Paleozoic İstanbul Zone (mainly arkosic sandstone) in some areas of the region. This sequence was named the Meşetepe Formation by Gedik et al. (2005) and the İstanbul Formation (Late Oligocene-Middle Miocene) by Özgül (2011). Sekmen (2019) explained that Neogene sand, gravel and clay levels are products of land erosion. Güngör et al. (2015) reported a clay-sand-coal sequence at the bottom of the basin and a thick sand layer above it and noted that the uppermost sand-clay sand levels of the basin are Pliocene in age. Some clays gained refractory properties due to the effect of humic acid entering the environment (Sipahi and Kuzum, 2011). Arkun (1985) reported the thickness of the Şile Neogene sequence as approximately 14-38 m. According to the researcher, the lower zone of 11-18 m (Hamamyatağı Formation) contains refractory clay, coal, clayey sand and binding clay levels, and the upper zone of 13-18 m (Domalı Formation) contains white and red sand layers. Recently, the thickness of the Oligo-Miocene sequence was reported as 10-35 m by Genç (2019). According to the researcher, there is a 7-31 m thick clay-rich zone containing one or two thin coal layers at the bottom, and a sand zone approximately 3-15 m thick at the top. Özdamar et al. (2007) reported that three thin coal seams were found in the middle and upper layers of the stratigraphic section in the Şile Region.



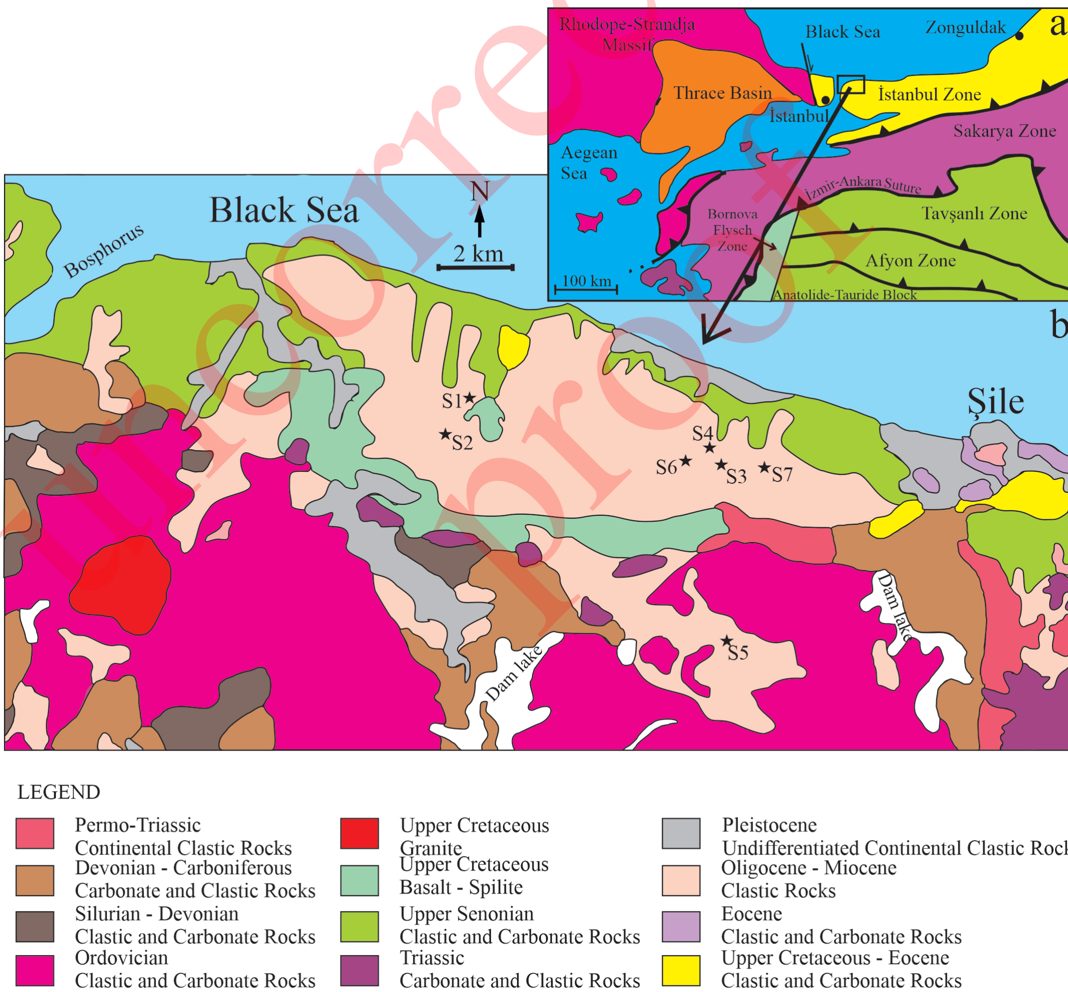


Figure 1- The location of the Şile Region in the tectonic units of northwestern Türkiye (Okay, and Kylander- Clark, 2023) and geology of the Şile Neogene Basin (ŞNB) and its surroundings (modified from the 1:250,000 scale geological map prepared by MTA, 2017).

## 3. Analytical Methods

In this study, 25 samples belonging to seven vertical sections (S1 to S7) in the ŞNB were analyzed mineralogically and chemically. Each vertical section also represents an open pit area where clay and sand production is actively occurring. Samples collected from each vertical section were numbered from bottom to top. Sample numbers based on sections are as follows: S1: 2, S2: 5; S3: 4, S4: 2, S5: 4, S6: 4, and S7: 4 samples.

The mineralogical compositions of the clay samples and their clay fractions were identified by X-ray diffraction (XRD) at the Istanbul Technical University using a Bruker D8 Advance instrument. The XRD analyses were performed with Ni-filtered CuKα radiation at a scanning speed of 1°2θ/min, a tube voltage of 40 kV, and current of 40 mA. Clay fractions of the samples (<2 µm) were prepared by using sedimentation and centrifuging. Oriented specimens on slides were analyzed after drying in air, solvated with ethylene glycol at 60°C for 16 h, and treated thermally at 350 °C and 550 °C for 2 h. Semi-quantitative mineralogical compositions of the samples were estimated by the XRD-reference intensity method (Chung, 1975) using the reference intensity constants of each component given by Ekinci-Şans et al. (2015). Furthermore, the mineral contents analyzed through XRD modal analyses of the clay samples were compared to their chemical compositions. Chemical analyses (X-ray fluorescence, XRF, and inductively coupled plasma-mass spectroscopy, ICP-MS) were performed at the İstanbul Technical University (ITU-JAL Laboratory). Pressed discs prepared using a wax binder and boric acid were analyzed by a Bruker S8 Tiger model XRF instrument. Trace-element concentrations were determined by using a Perkin Elmer Elan DRC-e 6100 ICP-MS instrument.

## 4. Results

### 4.1. Lithostratigraphy

ŞNB contains light-dark grey, beige, green, light brown, pink, and burgundy-colored clay levels, white, beige, grey, yellow, orange, and brick-colored sand levels and coal (lignite) levels and their transitional lithologies (Figures 2a-g). Seven vertical sections (S1 to S7) described lithostratigrapically in the basin (Figure 3). Figure 3 also shows sample points and numbers in each vertical section. Lithological thicknesses of the basin are presented in Table 1. In the south of the basin, S5 over the Paleozoic units is 6-12 km away from all other section points over the Mesozoic units. Compared to the others, S5 is at the highest topographic point (196 m), while other sections are at elevations between 114-164 m. The total apparent thickness of the sequence (sand, clay, clayey sand, sandy clay, clay with coal, clayey coal, coal) for all sections is between 8-44 m, and the average thickness is 25 m (Table 1). Thus, according to data from both the sections and some drilling, it is thought that the Neogene sediment thickness in the basin is < 54 m, and the average could be considered as 33 m.

The sand-clay transitions of the Neogene sequence show lateral differences. There is sand-rich lithology in some sections, while in others, there is clay-rich lithology (Figure 2a-f and Figure 3). Neogene deposits overlie on Paleozoic-aged arkoses in the south-southeast of the basin and have a total thickness of more than 20 m containing regularly recurring clay and sand levels with thicknesses of 2-4 m (Figure 2e and Figure 3). In the Neogene sequence located on Mesozoic-aged volcanics (andesite) in the center and east and northeast of the basin, there is a 15-20 m thick clay zone at the bottom and a 10-20 m thick sand zone at the top (Figures 2a, b, d and Figure 3). In some locations, clayey sand or sandy clay levels are within the lower clay zone (for example S2, S3 and S6). From south to north of the basin, the thickness of the Neogene sequence decreases and there is a transition from clay-rich lithology to sand-rich lithology. The upper sand zone reaches 25 m thick towards the basin's north.

The total clay and sand thicknesses that can be produced economically in the basin are between 0-21 m (average 12 m) and 4.5-17 m (average 9.5 m), respectively (Table 1). There is a minimum of 10 million m3 of clay reserves in 1 km2 in the basin. Conversely, the thicknesses of the clayey sand and sandy clay layers, typically not utilized in clay production, range from 0 to 11.5 meters, with an average thickness of 2 meters. While most sections contain two or three economically viable coal bands, some do not have any coal deposits. The total coal thickness varies from 0 to 1.2 meters, with an average of 0.3 meters. Additionally, the thickness of the unproduced clay coal or clayey coal ranges from 0 to 3.5 meters, averaging 0.6 meters.

### 4.2. Mineralogy

Modal-mineralogical compositions (XRD) of the clay samples from ŞNB is given in Table 2 (abbreviation for minerals after Whitney and Evans, 2010). Clay-mica minerals in the samples are kaolinite (15-60 %), illite

Table 1- Lithological thicknesses (m) obtained from field sections and maximum and average thicknesses (m) from field sections and drilling core data in the ŞNB (Total: sand + clay + clayey sand + sandy clay + clayey coal / clay with coal + coal).

| Lithology | Range of thickness (field sections) | Average thickness (field sections) | Maximum thickness (basin general) | Average thickness (basin general) |
|---|---|---|---|---|
| Sand | 4.5-17 | 9.5 | < 22 | 11 |
| Clay | 0-21 | 12 | < 30 | 11.5 |
| Clayey sand+sandy clay | 0-11.5 | 2 | < 16 | 2.5 |
| Clayey coal/clay with coal | 0-3.5 | 0.6 | < 3.5 | 1.3 |
| Coal | 0-1.2 | 0.3 | < 4 | 0.4 |
| Total | 8-44 | 25 | < 54 | 31 |

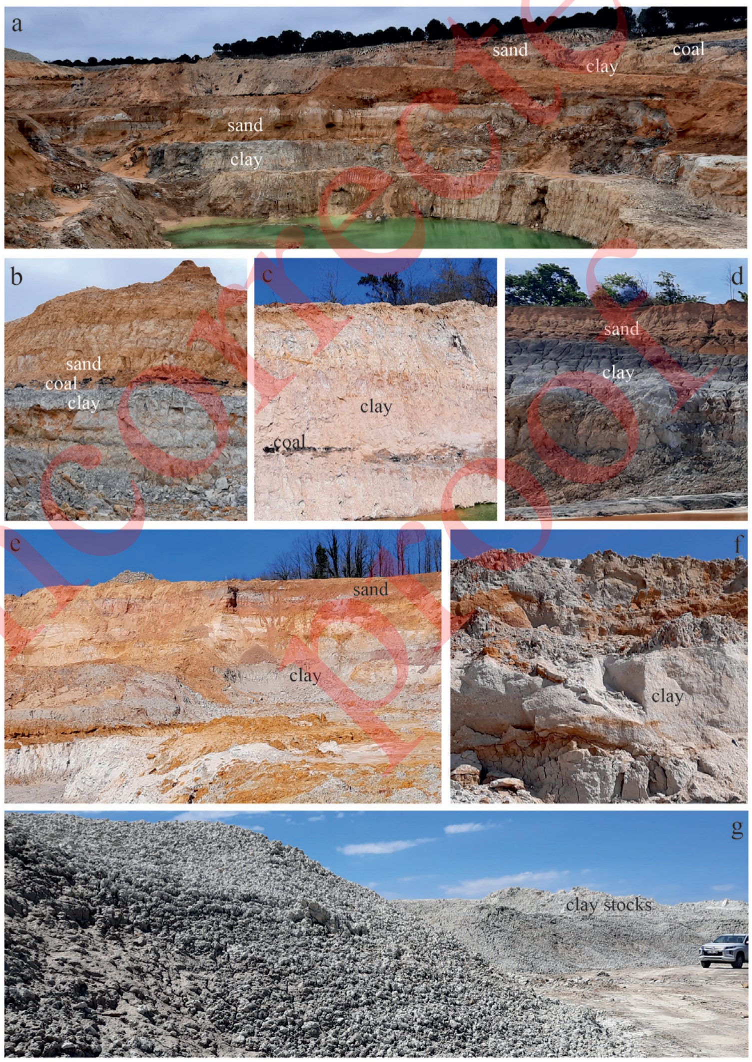


Figure 2- Field views of Şile Neogene Basin (ŞNB). a) Clay-sand alternation in the S1 pit area, b) Thick clay, fine coal and thick sand levels from bottom to top in the S2 pit area, c)Very thin irregular coal bands in the thick clay zone in the S3 pit area, d) Sand, light and dark gray colored clay and sand levels from bottom to top in the S6 pit area, e) White and gray clay levels with local iron oxide/hydroxide at the bottom and sand levels at the top in the S5 pit area, f) Close view of the clay level in the same quarry, g) Clay stocks in the S7 pit area.

(<25 %), Ca-smectite (<15 %), mixed layer phase (I/S; <5 %), chlorite (<5 %) and trace amount of muscovite (+/- sericite). Kaolinite is the only mineral found in all studied samples. Non-clay (- mica) minerals are quartz (<70 %), feldspar (<10 %), siderite (<10 %), anatase (<2 %), iron oxides/hydroxides (<4%), alunite (<2%) and pyrite (<3%). Other non-clay minerals, except for quartz, were found in minor or trace amounts in a few samples. Gypsum was detected in coal clay/clay coal and coal levels. Kaolinite, illite, Ca-smectite, mixed layer phase, quartz, gypsum and pyrite were detected in coal levels with very high amorphous components.

The whole-rock (WR) XRD traces of the studied samples are quite similar to each other. WR-XRD traces of three clay samples (S2-5, S5-1 and S6-1) with different mineral ratios and clay fraction-air dried (AD) and -high temperature (HT-550 °C) traces of the S2-5 are given in Figure 4. Kaolinite is evident in the XRD patterns with basal peaks of 7.1 Å and 3.56 Å, and collapsed after heating at 550 °C. Based on clay fraction data, the 10 Å phase in the samples is almost entirely illite, with muscovite (+/- sericite) rare. While Ca-smectite was found in all clay levels of some vertical sections, it was not detected in any level of some sections. The basal spacing of smectite (14-15 Å) in AD trace increases to 16-17 Å after ethylene glycol treatment and decreases to 9-10 Å after heating at 550 °C (and at 350 °C) and overlaps with illite (d001). The mixed layer phase detected in trace amounts in a few samples is the illite/smectite (I/S) phase.

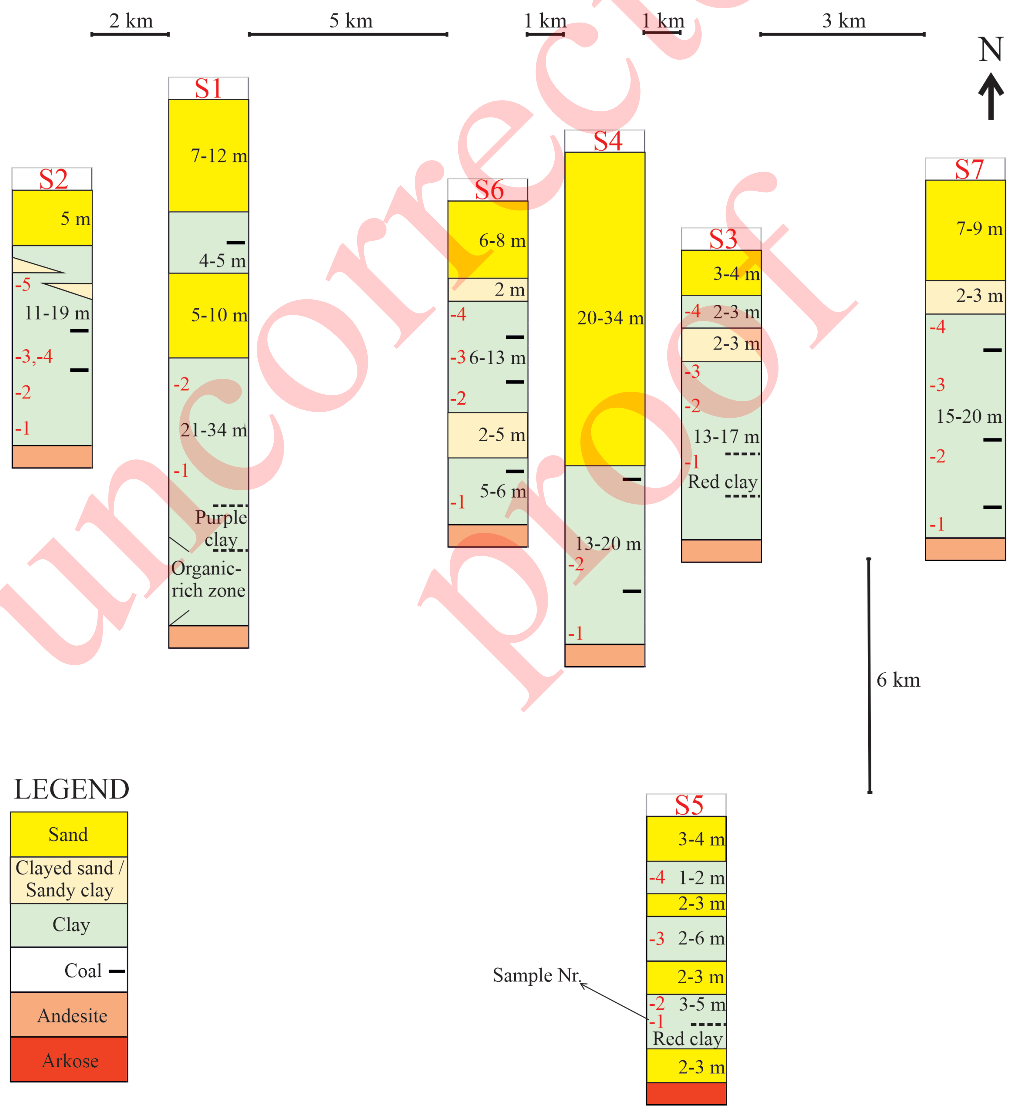


Figure 3- Measured stratigraphic sections (S1 to S7) of the ŞNB (not to scale; distances are approximate).

Table 2- Modal-mineralogical compositions of the clay samples from the ŞNB (by XRD, %; wt) (Kao: Kaolinite, Ilt-Mic: Illite-Mica, Sme: Smectite, Chl: Chlorite, ML: Mixed-Layer, (I/S: Illite/Smectite, Qz: Quartz, Fsp: Feldspar, Sd: Siderite, Ant: Anatase, Oxi/Hyd: Oxides/Hydroxides, Py: Pyrite, Alu: Alunite, abbreviations after Whitney and Evans, 2010).

| Sample | Kao | Ilt-Mic | Ca-Sme | Chl | ML (I/S) | Qz | Fsp | Sd | Ant | Fe-Oxi / Hyd | Py | Alu |
|---|---|---|---|---|---|---|---|---|---|---|---|---|
| S1-1 | 55-60 | 15-20 | - | - | - | 15-20 | <5 | 5-10 | <2 | - | - | - |
| S1-2 | 50-55 | 15-20 | - | - | - | 20-25 | <5 | <2 | <2 | <2 | - | - |
| S2-1 | 50-55 | 15-20 | - | - | - | 20-25 | 5-10 | <5 | <2 | - | - | - |
| S2-2 | 45-50 | 15-20 | - | - | - | 25-30 | 5-10 | <2 | <2 | <2 | - | - |
| S2-3 | 50-55 | 15-20 | <5 | - | - | 15-20 | 5-10 | <5 | <2 | - | - | - |
| S2-4 | 50-55 | 15-20 | - | - | - | 20-25 | 5-10 | <5 | <2 | - | - | - |
| S2-5 | 45-50 | 10-15 | - | - | - | 30-35 | <5 | <2 | <2 | <4 | - | <2 |
| S3-1 | 30-35 | 20-25 | <5 | - | <5 | 30-35 | <5 | <5 | <2 | - | - | - |
| S3-2 | 15-20 | <5 | 5-10 | <5 | - | 65-70 | - | <5 | <2 | - | - | - |
| S3-3 | 30-35 | 10-15 | 10-15 | <5 | - | 35-40 | <3 | - | <2 | - | - | - |
| S3-4 | 50-55 | 5-10 | 5-10 | - | - | 30-35 | - | - | - | - | - | - |
| S4-1 | 40-45 | 15-20 | 5-10 | <5 | - | 25-30 | <2 | - | <2 | - | - | - |
| S4-2 | 45-50 | 15-20 | <5 | - | - | 25-30 | <3 | - | <2 | - | - | - |
| S5-1 | 45-50 | 15-20 | - | - | - | 25-30 | <5 | - | <2 | - | - | |
| S5-2 | 45-50 | <5 | - | - | - | 50-55 | - | - | <2 | - | - | - |
| S5-3 | 35-40 | - | - | - | - | 60-65 | <5 | - | <2 | - | - | - |
| S5-4 | 35-40 | - | - | - | - | 55-60 | <5 | - | <2 | - | - | - |
| S6-1 | 55-60 | 10-15 | 5-10 | - | <5 | 15-20 | <2 | <2 | - | - | <2 | <2 |
| S6-2 | 45-50 | 15-20 | <5 | - | - | - | <5 | 5-10 | - | - | <3 | - |
| S6-3 | 15-20 | 10-15 | <5 | - | - | 60-65 | - | <5 | <2 | - | - | - |
| S6-4 | 30-35 | 10-15 | - | - | - | 50-55 | <5 | - | <2 | - | - | - |
| S7-1 | 50-55 | 20-25 | - | - | - | 20-25 | <5 | - | <2 | - | - | - |
| S7-2 | 50-55 | 20-25 | <5 | - | - | 20-25 | <2 | <2 | <2 | - | - | - |
| S7-3 | 50-55 | 15-20 | - | - | - | 20-25 | <2 | <2 | <2 | <2 | - | - |
| S7-4 | 50-55 | 20-25 | - | - | - | 15-20 | <5 | <2 | <2 | <4 | - | - |
| General | 15-60 | 0-25 | 0-15 | 0-5 | 0-5 | 0-70 | 0-10 | 0-10 | 0-2 | 0-4 | 0-3 | 0-2 |



4.3. Geochemistry

Geochemical analysis results (major oxides, trace, and rare earth elements) of the clay levels of ŞNB are presented in Tables 3, 4, and 5, and the average of some chemical values based on the sections are given in Tables 6 and 7. The ranges of major oxides are as follows; $SiO_2$: 49.90-71.30%, $Al_2O_3$: 16.63-30.57%, $Fe_2O_3$: 1.69-7.62%, $TiO_2$:1.04-1.72%, MgO: 0.39-1.04% and $K_2O$: 1.13-3.32%. ŞNB has low CaO (<0.37%) and $Na_2O$ (<0.13%) content (Table 3). LOIs are between 5.58 and 11.45%. For most major oxides and $SiO_2/Al_2O_3$ ratios, there is no significant vertical or lateral change in the basin. $K_2O$ is relatively low in S5 (Tables 3 and 6). $Fe_2O_3$ and sum of $Fe_2O_3$+MgO regularly decreases from the lower part to the middle–upper parts in the Neogene sequence for S2, S3, and S4. In contrast, it regularly increases for S7 and is variable for the other sections. The total trace elements in clay levels are 969-1662 ppm, and the Th/U ratio is 1.50-4.92 (Table 4). Total REE values range as follows. ΣREE: 50-443 ppm, ΣLREE: 14-331 ppm, ΣMREE: 2.8-31 ppm and ΣHREE: 29.1-80.8 ppm (Table 5).

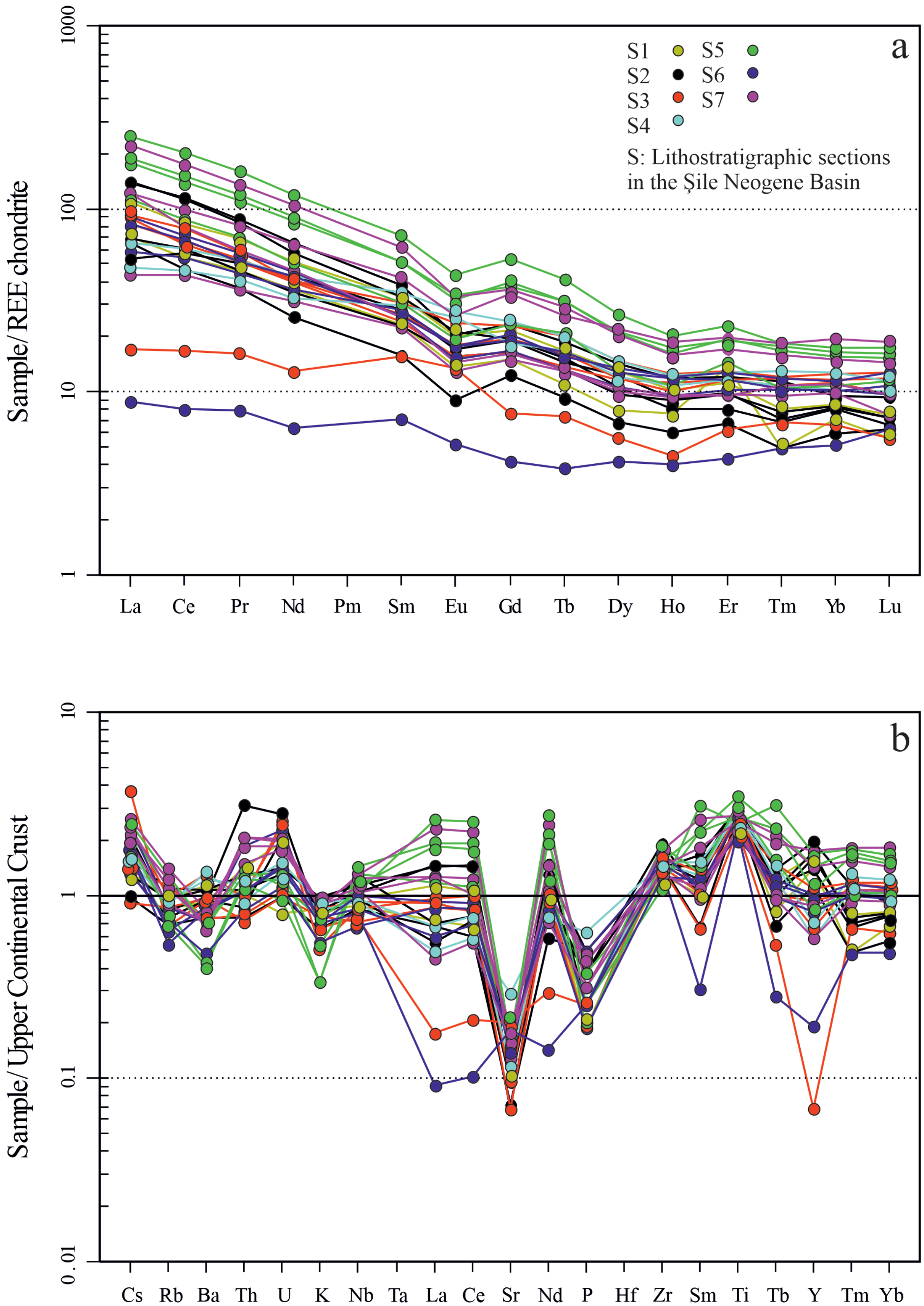


Figure 5- Normalized REE diagrams for the clay samples from the ŞNB. a) Upper continental crust (UCC) normalized (Taylor and McLennan 1995), b) Chondrite normalized (Boynton, 1984).

Table 3- Chemical analysis results of major oxides of the samples from clay levels in the ŞNB (samples are listed from bottom to top for each lithostratigraphic section - S).

| Major oxides (%) | S1-1 | S-1-2 | S2-1 | S2-2 | S2-3 | S2-4 | S2-5 | S3-1 | S3-2 | S3-3 | S3-4 | S4-1 | S4-2 | S5-1 | S5-2 | S5-3 | S5-4 | S6-1 | S6-2 | S6-3 | S6-4 | S7-1 | S7-2 | S7-3 | S7-4 |
|---|---|---|---|---|---|---|---|---|---|---|---|---|---|---|---|---|---|---|---|---|---|---|---|---|---|
| $SiO_2$ | 54.96 | 59.17 | 59.05 | 62.75 | 58.21 | 59.38 | 61.28 | 67.58 | 69.35 | 60.08 | 53.64 | 57.82 | 58.26 | 58.92 | 59.59 | 71.30 | 71.05 | 49.90 | 50.82 | 67.58 | 61.22 | 60.04 | 56.71 | 56.32 | 54.73 |
| $Al_2O_3$ | 24.84 | 25.87 | 24.58 | 23.62 | 25.55 | 24.67 | 23.65 | 16.94 | 16.72 | 23.95 | 30.57 | 25.53 | 25.53 | 24.62 | 21.98 | 17.01 | 18.09 | 27.62 | 24.87 | 16.63 | 25.4 | 25.73 | 26.54 | 24.84 | 24.93 |
| $Fe_2O_3$ | 6.16 | 2.56 | 4.24 | 2.43 | 2.30 | 3.40 | 4.61 | 4.72 | 3.64 | 3.35 | 2.04 | 3.02 | 2.87 | 3.25 | 6.52 | 2.09 | 1.69 | 5.42 | 7.62 | 5.29 | 1.95 | 1.93 | 2.77 | 4.69 | 7.12 |
| MnO | 0.03 | 0.02 | 0.02 | 0.02 | 0.01 | 0.01 | 0.01 | 0.03 | 0.02 | 0.01 | 0.01 | 0.01 | 0.02 | 0.01 | 0.01 | 0.01 | 0.01 | 0.02 | 0.04 | 0.05 | 0.01 | 0.01 | 0.02 | 0.05 | 0.01 |
| $TiO_2$ | 1.36 | 1.34 | 1.39 | 1.48 | 1.51 | 1.54 | 1.36 | 1.22 | 1.16 | 1.48 | 1.13 | 1.43 | 1.42 | 1.25 | 1.35 | 1.72 | 1.55 | 1.11 | 1.04 | 1.07 | 1.33 | 1.36 | 1.18 | 1.26 | 1.14 |
| MgO | 0.63 | 0.58 | 0.53 | 0.56 | 0.67 | 0.54 | 0.45 | 0.82 | 0.75 | 0.99 | 0.78 | 0.93 | 0.82 | 0.80 | 0.66 | 0.46 | 0.39 | 0.89 | 0.83 | 0.87 | 0.75 | 0.93 | 1.04 | 1.01 | 0.82 |
| CaO | 0.14 | 0.20 | 0.10 | 0.07 | 0.08 | 0.07 | 0.05 | 0.21 | 0.26 | 0.06 | 0.06 | 0.22 | 0.18 | 0.22 | 0.20 | 0.14 | 0.11 | 0.34 | 0.37 | 0.33 | 0.13 | 0.19 | 0.17 | 0.27 | 0.17 |
| $K_2O$ | 2.86 | 2.57 | 2.42 | 2.64 | 3.32 | 2.81 | 2.20 | 2.58 | 1.77 | 2.85 | 2.22 | 2.77 | 3.06 | 2.54 | 1.81 | 1.13 | 1.13 | 2.37 | 2.53 | 1.88 | 2.35 | 2.85 | 3.12 | 3.00 | 3.00 |
| $Na_2O$ | 0.10 | 0.07 | 0.06 | 0.07 | 0.08 | 0.07 | 0.07 | 0.07 | 0.09 | 0.10 | 0.09 | 0.11 | 0.10 | 0.07 | 0.07 | 0.05 | 0.05 | 0.13 | 0.1 | 0.1 | 0.11 | 0.08 | 0.09 | 0.10 | 0.11 |
| $P_2O_5$ | 0.04 | 0.03 | 0.06 | 0.06 | 0.04 | 0.08 | 0.08 | 0.03 | 0.03 | 0.04 | 0.04 | 0.10 | 0.04 | 0.04 | 0.06 | 0.03 | 0.04 | 0.04 | 0.03 | 0.08 | 0.04 | 0.05 | 0.05 | 0.07 | 0.07 |
| $SO_3$ | 0.02 | 0.18 | 0.05 | 0.16 | 0.17 | 0.05 | 0.07 | 0.06 | 0.05 | 0.04 | 0.04 | 0.06 | 0.13 | 0.02 | 0.03 | 0.02 | 0.02 | 0.57 | 0.20 | 0.05 | 0.17 | 0.06 | 0.12 | 0.10 | 0.04 |
| Cl | 0.01 | 0.02 | 0.02 | 0.02 | 0.01 | 0.02 | 0.03 | 0.01 | 0.01 | 0.01 | 0.01 | 0.01 | 0.01 | 0.01 | 0.01 | 0.01 | 0.01 | 0.01 | 0.01 | 0.01 | 0.01 | 0.01 | 0.01 | 0.01 | 0.01 |
| Cr2O3 | 0.02 | 0.02 | 0.02 | 0.01 | 0.02 | 0.02 | 0.01 | 0.01 | 0.01 | 0.01 | 0.01 | 0.01 | 0.01 | 0.01 | 0.02 | 0.01 | 0.01 | 0.01 | 0.01 | 0.01 | 0.01 | 0.01 | 0.24 | 0.49 | 0.02 |
| LOI | 8.68 | 7.23 | 7.31 | 5.98 | 7.87 | 7.19 | 6.00 | 5.58 | 5.99 | 6.90 | 9.23 | 7.80 | 7.39 | 8.10 | 7.56 | 5.91 | 5.74 | 11.45 | 11.42 | 5.96 | 6.41 | 6.63 | 7.83 | 7.67 | 7.71 |
| $SiO_2/Al_2O_3$ | 2.21 | 2.29 | 2.40 | 2.66 | 2.28 | 2.41 | 2.59 | 3.99 | 4.15 | 2.51 | 1.75 | 2.26 | 2.28 | 2.39 | 2.71 | 4.19 | 3.93 | 1.81 | 2.04 | 4.06 | 2.41 | 2.33 | 2.14 | 2.27 | 2.20 |
| $Fe_2O_3$+MgO | 6.79 | 3.14 | 4.77 | 2.99 | 2.97 | 3.94 | 5.06 | 5.54 | 4.39 | 4.34 | 2.82 | 3.95 | 3.69 | 4.05 | 7.18 | 2.55 | 2.08 | 6.31 | 8.45 | 6.16 | 2.70 | 2.86 | 3.81 | 5.70 | 7.94 |

Table 4- Trace element values of the samples from clay levels in the ŞNB (samples are listed from bottom to top for each lithostratigraphic section - S).

| Trace elements (ppm) | S1-1 | S-1-2 | S2-1 | S2-2 | S2-3 | S2-4 | S2-5 | S3-1 | S3-2 | S3-3 | S3-4 | S4-1 | S4-2 | S5-1 | S5-2 | S5-3 | S5-4 | S6-1 | S6-2 | S6-3 | S6-4 | S7-1 | S7-2 | S7-3 | S7-4 |
|---|---|---|---|---|---|---|---|---|---|---|---|---|---|---|---|---|---|---|---|---|---|---|---|---|---|
| As | 4 | 3 | <1 | <1 | <1 | <1 | 8 | 9 | 10 | 10 | 16 | 8 | 10 | 11 | 21 | 16 | 13 | 23 | 23 | 13 | 12 | 15 | 12 | 11 | 18 |
| Ba | 616 | 512 | 540 | 513 | 586 | 584 | 413 | 526 | 717 | 404 | 516 | 739 | 667 | 376 | 373 | 233 | 225 | 455 | 471 | 264 | 391 | 366 | 390 | 396 | 452 |
| Co | 6 | 9 | 10 | 10 | 28 | 4 | 8 | 18 | 9 | 10 | 6 | 7 | 9 | 6 | 10 | 3 | 1 | 10 | 11 | 14 | 9 | 4 | 11 | 10 | 9 |
| Cs | 4.92 | 6.49 | 7.78 | 4.82 | 5.81 | 4.73 | 3.60 | 3.38 | 8.92 | 5.02 | 13.89 | 5.82 | 6.24 | 9.28 | 7.90 | 6.96 | 6.08 | 6.31 | 6.45 | 4.93 | 8.70 | 8.03 | 7.29 | 8.68 | 9.77 |
| Cu | 35 | 34 | 48 | 33 | 35 | 20 | 34 | 21 | 17 | 17 | 19 | 35 | 31 | 19 | 32 | 12 | 8 | 50 | 53 | 28 | 27 | 31 | 39 | 36 | 25 |
| Ga | 24.86 | 21.41 | 22.61 | 19.34 | 28.74 | 28.51 | 20.61 | 16.21 | 16.78 | 24.96 | 21.24 | 20.73 | 23.96 | 28.31 | 22.79 | 20.83 | 16.82 | 30.32 | 24.65 | 15.18 | 24.09 | 29.37 | 27.03 | 32.17 | 30.61 |
| In | 0.02 | 0.01 | 0.04 | 0.01 | 0.01 | 0.01 | 0.01 | 0.01 | 0.01 | 0.03 | 0.01 | 0.01 | 0.01 | 0.01 | 0.01 | 0.01 | 0.01 | 0.01 | 0.01 | 0.01 | 0.01 | 0.01 | 0.01 | 0.01 | 0.01 |
| Mo | 1 | 1 | 1 | 1 | 3 | 1 | 1 | 1 | <1 | <1 | 4 | 1 | <1 | 1 | 1 | 1 | 1 | 2 | 2 | 1 | <1 | 2 | 3 | 2 | 1 |
| Nb | 22 | 24 | 32 | 24 | 28 | 26 | 21 | 18 | 21 | 23 | 19 | 23 | 24 | 26 | 28 | 36 | 33 | 20 | 21 | 17 | 25 | 32 | 27 | 31 | 26 |
| Ni | 51 | 52 | 37 | 44 | 60 | 33 | 44 | 34 | 34 | 27 | 50 | 41 | 37 | 35 | 41 | 19 | 17 | 51 | 50 | 36 | 34 | 33 | 45 | 50 | 42 |
| Pb | 6 | 26 | 22 | 10 | 27 | 23 | 12 | 28 | 36 | 27 | 67 | 42 | 49 | 38 | 52 | 28 | 24 | 17 | 16 | 15 | 13 | 46 | 36 | 39 | 38 |
| Rb | 106.8 | 94.4 | 92.5 | 84.7 | 122.6 | 106.9 | 77.3 | 95.6 | 109.4 | 125.6 | 75.8 | 100.1 | 102.6 | 143.2 | 124.7 | 91.4 | 77.2 | 61.0 | 71.8 | 80.5 | 96.1 | 136.8 | 99.8 | 122.0 | 157.8 |
| Sc | 24 | 23 | 17 | 19 | 23 | 22 | 19 | 18 | 21 | 14 | 22 | 22 | 22 | 22 | 20 | 16 | 13 | 25 | 22 | 16 | 22 | 18 | 21 | 16 | 19 |
| Sr | 35 | 34 | 33 | 24 | 34 | 45 | 25 | 24 | 34 | 68 | 70 | 101 | 41 | 58 | 55 | 54 | 47 | 64 | 56 | 53 | 48 | 46 | 56 | 58 | 64 |
| Th | 10.93 | 15.06 | 33.21 | 9.17 | 13.76 | 11.50 | 8.09 | 7.81 | 10.52 | 8.38 | 10.79 | 9.84 | 12.25 | 15.05 | 13.73 | 13.07 | 12.33 | 11.30 | 11.34 | 8.91 | 19.80 | 22.26 | 15.84 | 22.16 | 19.84 |
| Tl | 0.89 | 0.95 | 1.10 | 1.01 | 1.02 | 0.80 | 0.55 | 0.65 | 0.98 | 0.85 | 1.50 | 0.84 | 0.89 | 1.14 | 0.96 | 0.87 | 0.85 | 0.85 | 0.63 | 0.50 | 1.10 | 1.08 | 0.99 | 1.17 | 1.24 |
| U | 2.22 | 5.51 | 7.76 | 5.65 | 3.94 | 3.69 | 2.73 | 2.75 | 7.00 | 2.93 | 6.46 | 3.64 | 4.22 | 3.17 | 3.73 | 3.38 | 2.62 | 3.93 | 4.08 | 3.11 | 6.40 | 5.52 | 5.04 | 5.74 | 5.17 |
| V | 147 | 134 | 124 | 118 | 123 | 136 | 114 | 86 | 98 | 106 | 100 | 106 | 119 | 137 | 132 | 111 | 96 | 131 | 113 | 97 | 117 | 125 | 115 | 137 | 133 |
| Y | 31.05 | 35.82 | 34.96 | 37.65 | 42.74 | 30.36 | 24.90 | 23.79 | 14.53 | 20.36 | 1.51 | 12.73 | 15.42 | 37.25 | 23.43 | 31.40 | 18.18 | 4.17 | 21.40 | 22.35 | 17.76 | 31.57 | 12.82 | 38.61 | 19.07 |
| Zn | 63 | 67 | 27 | 51 | 122 | 36 | 44 | 93 | 88 | 107 | 68 | 137 | 127 | 86 | 82 | 47 | 33 | 76 | 87 | 71 | 89 | 78 | 63 | 85 | 57 |
| Zr | 245 | 271 | 365 | 286 | 268 | 280 | 276 | 309 | 278 | 272 | 268 | 281 | 288 | 206 | 217 | 287 | 355 | 258 | 240 | 285 | 323 | 331 | 257 | 274 | 242 |
| Σ Trace elements | 1382 | 1311 | 1404 | 1239 | 1490 | 1344 | 1113 | 1293 | 1496 | 1239 | 1333 | 1662 | 1552 | 1199 | 1218 | 983 | 969 | 1271 | 1262 | 1007 | 1244 | 1312 | 1210 | 1321 | 1331 |

Table 5- Rare earth element values of the samples from clay levels in the ŞNB (samples are listed from bottom to top for each lithostratigraphic section - S).

| REE (ppm) | S1-1 | S-1-2 | S2-1 | S2-2 | S2-3 | S2-4 | S2-5 | S3-1 | S3-2 | S3-3 | S3-4 | S4-1 | S4-2 |
|---|---|---|---|---|---|---|---|---|---|---|---|---|---|
| La | 21.73 | 33.75 | 21.20 | 16.49 | 43.06 | 43.70 | 20.21 | 25.58 | 28.83 | 27.39 | 5.31 | 14.80 | 20.15 |
| Ce | 43.58 | 67.02 | 48.82 | 46.17 | 93.12 | 92.14 | 38.00 | 53.18 | 63.64 | 51.80 | 13.47 | 37.44 | 49.01 |
| Pr | 5.59 | 8.47 | 5.58 | 6.17 | 10.71 | 10.33 | 4.53 | 6.47 | 7.08 | 6.25 | 1.96 | 5.05 | 6.43 |
| Nd | 21.63 | 30.80 | 21.04 | 25.53 | 38.78 | 34.27 | 15.24 | 24.14 | 24.38 | 24.00 | 7.73 | 19.58 | 25.78 |
| Sm | 4.56 | 6.42 | 4.48 | 5.48 | 7.45 | 6.49 | 3.07 | 6.00 | 5.14 | 4.68 | 3.01 | 5.78 | 6.85 |
| Eu | 1.01 | 1.47 | 1.14 | 1.25 | 1.51 | 1.55 | 0.66 | 1.74 | 1.33 | 1.15 | 0.99 | 1.87 | 2.02 |
| Gd | 3.88 | 5.60 | 4.29 | 4.93 | 6.07 | 5.03 | 3.16 | 5.88 | 5.00 | 4.28 | 1.97 | 4.78 | 6.21 |
| Tb | 0.52 | 0.79 | 0.62 | 0.68 | 0.88 | 0.73 | 0.44 | 0.95 | 0.77 | 0.65 | 0.35 | 0.79 | 0.96 |
| Dy | 2.54 | 4.17 | 3.12 | 3.96 | 4.57 | 3.40 | 2.18 | 4.76 | 3.82 | 3.76 | 1.81 | 3.86 | 4.71 |
| Ho | 0.55 | 0.73 | 0.65 | 0.66 | 0.85 | 0.58 | 0.43 | 0.89 | 0.72 | 0.81 | 0.32 | 0.77 | 0.88 |
| Er | 2.86 | 2.37 | 2.02 | 2.07 | 2.51 | 1.70 | 1.41 | 2.74 | 2.46 | 2.43 | 1.31 | 2.44 | 2.68 |
| Tm | 0.16 | 0.26 | 0.25 | 0.23 | 0.37 | 0.22 | 0.16 | 0.39 | 0.38 | 0.35 | 0.22 | 0.35 | 0.42 |
| Yb | 1.48 | 1.79 | 1.75 | 1.71 | 2.00 | 1.69 | 1.24 | 2.59 | 2.44 | 2.36 | 1.38 | 2.13 | 2.66 |
| Lu | 0.18 | 0.24 | 0.23 | 0.23 | 0.30 | 0.21 | 0.20 | 0.41 | 0.38 | 0.31 | 0.18 | 0.32 | 0.37 |
| Σ REE | 165 | 223 | 167 | 172 | 278 | 254 | 135 | 178 | 182 | 165 | 64 | 135 | 167 |
| Σ LREE | 93 | 140 | 97 | 94 | 186 | 181 | 78 | 109 | 124 | 109 | 29 | 77 | 101 |
| Σ MREE | 9.5 | 13.5 | 9.9 | 11.7 | 15.0 | 13.1 | 6.9 | 13.6 | 11.5 | 10.1 | 6.0 | 12.4 | 15.1 |
| Σ HREE | 63.3 | 69.2 | 60.6 | 66.2 | 77.2 | 60.9 | 50.0 | 54.5 | 46.5 | 45.0 | 29.1 | 45.4 | 50.1 |
| Eu/Eu* | 1.05 | 1.08 | 1.14 | 1.06 | 0.98 | 1.19 | 0.93 | 1.29 | 1.15 | 1.13 | 1.76 | 1.56 | 1.36 |
| Ce/Ce* | 0.19 | 0.19 | 0.21 | 0.19 | 0.21 | 0.22 | 0.20 | 0.20 | 0.22 | 0.20 | 0.17 | 0.19 | 0.19 |
| Yb/Yb* | 1.37 | 1.13 | 1.15 | 1.17 | 0.95 | 1.24 | 1.09 | 1.02 | 1.01 | 1.13 | 1.09 | 1.01 | 1.07 |
| $La_N/Yb_N$ | 1.42 | 1.83 | 1.17 | 0.93 | 2.09 | 2.50 | 1.58 | 0.96 | 1.14 | 1.12 | 0.37 | 0.67 | 0.73 |

| REE (ppm) | S5-1 | S5-2 | S5-3 | S5-4 | S6-1 | S6-2 | S6-3 | S6-4 | S7-1 | S7-2 | S7-3 | S7-4 |
|---|---|---|---|---|---|---|---|---|---|---|---|---|
| La | 76.79 | 55.62 | 58.08 | 35.36 | 2.73 | 17.99 | 25.78 | 27.89 | 68.98 | 13.50 | 37.79 | 37.54 |
| Ce | 163.13 | 113.64 | 122.78 | 70.61 | 6.51 | 44.00 | 54.26 | 57.85 | 142.57 | 35.22 | 79.66 | 64.96 |
| Pr | 19.68 | 13.43 | 14.44 | 8.61 | 0.96 | 5.44 | 6.28 | 6.94 | 16.67 | 4.39 | 9.95 | 7.26 |
| Nd | 71.79 | 51.50 | 54.87 | 30.50 | 3.79 | 21.70 | 25.84 | 27.07 | 63.57 | 18.63 | 38.14 | 27.45 |
| Sm | 13.88 | 10.10 | 10.03 | 6.00 | 1.38 | 5.44 | 5.03 | 5.00 | 11.92 | 4.35 | 8.25 | 4.95 |
| Eu | 3.18 | 2.48 | 2.33 | 1.43 | 0.38 | 1.31 | 1.29 | 1.10 | 2.44 | 0.95 | 1.93 | 1.06 |
| Gd | 13.89 | 9.70 | 10.31 | 6.02 | 1.07 | 5.35 | 4.97 | 4.38 | 9.43 | 3.87 | 8.89 | 4.16 |
| Tb | 1.97 | 1.48 | 1.49 | 0.99 | 0.18 | 0.74 | 0.78 | 0.63 | 1.37 | 0.61 | 1.23 | 0.62 |
| Dy | 8.56 | 6.68 | 6.90 | 4.15 | 1.34 | 4.33 | 4.06 | 3.40 | 6.65 | 3.24 | 7.16 | 3.37 |
| Ho | 1.44 | 1.17 | 1.25 | 0.77 | 0.29 | 0.87 | 0.85 | 0.68 | 1.13 | 0.67 | 1.35 | 0.70 |
| Er | 4.78 | 4.08 | 4.01 | 3.06 | 0.90 | 2.68 | 2.46 | 2.15 | 3.60 | 2.04 | 4.13 | 1.99 |
| Tm | 0.59 | 0.54 | 0.57 | 0.34 | 0.16 | 0.38 | 0.34 | 0.33 | 0.51 | 0.31 | 0.60 | 0.35 |
| Yb | 3.64 | 3.26 | 3.41 | 2.27 | 1.06 | 2.38 | 2.10 | 2.12 | 3.13 | 2.04 | 4.04 | 2.29 |
| Lu | 0.56 | 0.49 | 0.52 | 0.37 | 0.20 | 0.41 | 0.35 | 0.31 | 0.47 | 0.24 | 0.60 | 0.31 |
| Σ REE | 443 | 318 | 338 | 202 | 50 | 156 | 173 | 180 | 382 | 124 | 258 | 195 |
| Σ LREE | 331 | 234 | 250 | 145 | 14 | 89 | 112 | 120 | 292 | 72 | 166 | 137 |
| Σ MREE | 31.0 | 22.3 | 22.7 | 13.5 | 2.8 | 12.1 | 11.3 | 10.5 | 23.8 | 9.2 | 19.1 | 10.2 |
| Σ HREE | 80.8 | 61.1 | 65.5 | 43.1 | 33.3 | 55.2 | 49.3 | 49.4 | 66.4 | 43.0 | 73.7 | 47.7 |
| Eu/Eu* | 1.00 | 1.10 | 1.00 | 1.04 | 1.37 | 1.07 | 1.13 | 1.03 | 1.01 | 1.02 | 0.99 | 1.02 |
| Ce/Ce* | 0.20 | 0.21 | 0.21 | 0.20 | 0.17 | 0.20 | 0.21 | 0.20 | 0.21 | 0.20 | 0.20 | 0.21 |
| Yb/Yb* | 1.00 | 1.00 | 0.99 | 1.01 | 0.93 | 0.95 | 0.96 | 1.05 | 1.01 | 1.18 | 1.06 | 1.10 |
| $La_N/Yb_N$ | 2.04 | 1.65 | 1.65 | 1.51 | 0.25 | 0.73 | 1.19 | 1.27 | 2.13 | 0.64 | 0.91 | 1.59 |

The whole-rock trace and REE contents of clay samples from the ŞNB were normalized to upper continental crust (UCC) (Taylor and McLennan, 1995) and to chondrite (Boynton, 1984). The trace-element profile of the ŞNB's clay levels illustrates homogeneity and is compatible with the average UCC except for the Ba, Th, Sr, P and Zr contents (Figure 5). Th/U ratios of the ŞNB's clay samples (1.50-4.92) are similar to the average Th/U ratio of the UCC of 3.8 (Condie, 1993; Taylor and McLennan, 1995). On the other hand, there is a significant chemical difference between the lower and the upper clay levels in the ŞNB. S1-1, S1-2, S2-1, S3-2, and S7-1 are the samples from the bottom levels, and S2-6, S3-5, S6-5, and S7-5 are from the upper levels. Only As, Cs, and Sr are relatively high in the upper clay levels. In contrast, Cu, Nb, Pb, Th, Y, Zr, Th/U, ΣREE, ΣLREE, ΣMREE, and ΣHREE are significantly higher in lower clay levels (Tables 4 and 5). The Th/U ratio is highest in the lowest clay levels close to the bedrock (Samples S1-1, S2-1, S5-1, and S7-1 in Table 4). In some areas, the lowest clay levels in the basin most likely formed because of in-situ alteration of andesite. Therefore, the clay levels' relatively high Th/U ratio indicates volcanic effect.

In S1, there is an increase in REE lithostratigrapically from bottom to top (samples S1-1 and S1-2) (Table 5). There is no significant difference in the total trace element value. In S2, there is an increase in REE from the lowest clay level (sample S2-1) to the middle level (samples S2-2 and S2-3). However, it decreases relatively at the upper levels (samples S2-4 and S2-5). This section has the highest LREE (La-Sm) values in the basin. There is a decrease in trace elements from bottom to top in S2. In S3, REE values decrease from bottom to top. The top clay level (sample S3-4) has very low REE values. The uppermost clay levels of S2 and S3 have the lowest HREE (Eu-Lu) values in the basin. There is no significant change in trace elements in S3. In S4, sample S4-1 is at the bottom, a gray clay sample under coal, and sample S4-2 is a dark gray clay sample above coal. REE values increase from bottom to top. This section has the highest values for Eu-Lu in the entire basin (REE-chondrite diagram; Boynton, 1984). There is a decrease in total trace element value from bottom to top.

ΣREE in clay samples of S5, a Neogene section over the Paleozoic aged sandstones (arkose), is between 202-443 ppm and the average is 325 ppm. In S5, ΣREE, ΣLREE (145-331 ppm; with average of 240 ppm), ΣMREE (13.5-31.0 ppm; with average of 22.4 ppm), ΣHREE (43.1-80.8 ppm; with average of 62.6 ppm) and LaN/YbN ratio are higher than those of clay samples from the Neogene section are over the Mesozoic aged andesitic volcanic rocks (Tables 6 and 7). Only the Eu/Eu* ratio is relatively low in Neogene clays over the Paleozoic (Table 7). On the other hand, in S5, REE values are highest in the lowest clay level (sample S5-1). This clay level is above a sand level overlying the Paleozoic arkoses. The sand level at the bottom (2-3 m) is laterally transitional and sometimes appears limonitized. The upper clay level has the lowest ΣREE of the section. It concluded that there is a decrease in REE values from bottom to top for S5 (from sample S5-1 to S5-4) and the total trace elements.

Table 6- The average values (ppm) of some chemical parameters based on lithostratigraphic sections in the ŞNB.

| Chemistry | S1 | S2 | S3 | S4 | S5 | S6 | S7 |
|---|---|---|---|---|---|---|---|
| $K_2O$ (%) | 2.72 | 2.68 | 2.36 | 2.92 | 1.65 | 2.28 | 2.99 |
| **Σ**Trace Elements | 1347 | 1318 | 1340 | 1607 | 1092 | 1196 | 1294 |
| Th/U | 3.83 | 3.09 | 2.22 | 2.80 | 4.25 | 2.90 | 3.72 |
| ΣREE | 194 | 201 | 147 | 151 | 325 | 140 | 240 |
| ΣLREE | 117 | 127 | 93 | 89 | 240 | 84 | 167 |
| ΣMREE | 11.5 | 11.3 | 10.3 | 13.8 | 22.4 | 9.2 | 15.6 |
| ΣHREE | 66.3 | 63.0 | 43.8 | 47.8 | 62.6 | 46.8 | 57.7 |
| Eu/Eu* | 1.07 | 1.06 | 1.19 | 1.56 | 1.04 | 1.15 | 1.01 |
| Ce/Ce* | 0.19 | 0.21 | 0.21 | 0.18 | 0.21 | 0.20 | 0.21 |
| Yb/Yb* | 1.25 | 1.12 | 1.05 | 1.06 | 1.00 | 0.97 | 1.09 |
| LaN/YbN | 1.63 | 1.65 | 1.07 | 0.59 | 1.71 | 0.86 | 1.32 |

Table 7- Comparison of range and average values (ppm) for some chemical parameters of Neogene lithostratigraphic sections over the Paleozoic and Mesozoic in the ŞNB.

| Chemistry | Neogene over Paleozoic (S5) | | Neogene over Mesozoic (S1-S4,S6,S7 | |
|---|---|---|---|---|
| | Range | Average | Range | Average |
| $K_2O$ (%) | 1.13–2.54 | 1.65 | 1.77–3.32 | 2.66 |
| ΣTrace Elements | 969–1218 | 1092 | 1007–1662 | 1350 |
| Th/U | 3.68–4.75 | 4.25 | 1.50–4.92 | 3.09 |
| ΣREE | 202–443 | 325 | 50–382 | 179 |
| ΣLREE | 145–331 | 240 | 14–292 | 113 |
| ΣMREE | 13.5–31.0 | 22.4 | 2.8–23.8 | 12.0 |
| ΣHREE | 43.1–80.8 | 62.6 | 29.1–77.2 | 54.2 |
| Eu/Eu* | 1.00–1.10 | 1.04 | 0.98–1.76 | 1.17 |
| Ce/Ce* | 0.20–0.21 | 0.21 | 0.17–0.22 | 0.20 |
| Yb/Yb* | 0.99–1.01 | 1.00 | 0.93–1.37 | 1.09 |
| LaN/YbN | 1.51–2.04 | 1.71 | 0.25–2.50 | 1.19 |

In S6, REE increases from bottom to top (samples S6-1 to S6-4; Table 5) (REE-chondrite diagram; Boynton, 1984). Interestingly, the lowest clay level of the section with high kaolinite content (sub-coal gray clay) has very low REE values. S6 has the basin's lowest trace element and REE values (UCC diagram; Taylor and McLennan, 1995 and REE-chondrite diagram; Boynton, 1984). The lowest clay level of S7 (sample S7-1) has very high REE values. This whitish-gray-colored level is an in-situ level formed by the in-situ weathering of Mesozoic-aged volcanics (andesite) at the bottom of the Neogene Basin. In the section, REE values decreased towards the middle level (sample S7-2), increased at the top (sample S7-3), and decreased above that (sample S7-4) (Table 5). There is no significant change in trace elements on a vertical scale.

## 5. Discussion

From a geochemical perspective, significant variations in clay levels within the ŞNB are reflected in the REE values (Tables 5, 6, and 7). Two key findings emerged from this context: 1) The clay levels associated with the Neogene sequence over Paleozoic-aged units exhibit considerably higher REE values than those found in the Neogene over Mesozoic-aged units. This finding also highlights a geographical distinction. While no significant variation in chemical values is observed in the east-west direction of the basin, there is a partial difference in the north-south direction. The highest REE values are in the south; 2) Whether on Paleozoic (arkoses) or Mesozoic (andesites), the REE values of the lower clay levels of the Neogene sequence are significantly higher than the upper-level clays.

Trace elements and REE values are relatively high in the west and northwest (S1 and S2) and easternmost (S7) of the basin, whereas they are lowest in an area of approximately 4 $km^2$ in the center (S3, S4 and S6). REEs show lateral and vertical differences throughout the basin. Canberk (2002) explained that Hf, Zr and Nb are mobile during the alteration process of andesitic volcanic rocks, whereas Ho, Er and Yb are immobile in the Şile region. Also, Norouzi et al. (2021) explained Hf enrichment and, on the other hand, partial depletion in many elements during the kaolinization process of andesitic rocks (NE Iran). However, element enrichment in sedimentary kaolin formations may not be directly related to kaolinite. For example, the REE (especially LREE) enrichment in in a heavy mineral subfraction from sedimantary kaolin deposit reported from Georgia (USA) (Boxleiter and Elliott, 2023). Our geochemical results show no significant differences in Hf, Zr, and Nb values, while there are lateral and vertical differences in Ho, Er, and Yb. Moreover, while the average sum of Ho+Er+Yb in Neogene clays over the Paleozoic is 9.56 ppm, it is 5.18 ppm on average in the Neogene clays over the Mesozoic.

Trace element and REE values of the ŞNB are considerably higher in clay than in sand levels. Although not the subject of this study, chemical analyses of samples taken from some sand levels in the basin were also performed. The sum of the trace element and REE of sand samples with $SiO_2$ values between 74-96% are between 200-1000 ppm and 20-120 ppm, respectively. The increase in REE is related mainly to the clay ratio in the sand. Koç et al. (2013) stated that the source of quartz sands in the Şile region are mostly quartz-rich sandstones. According to the authors, there are two groups of samples; in one group; Rb, Sr, Ba, and Ni are high, Zr is low, and in the other group, the opposite is true. The authors also stated that the group with higher Ni may be derived from ultrabasic-basic rocks, and the second group with high Zr may be derived from granitic rocks. On the other hand, major oxide and trace element values of coal bands (+ coal clay and clayey coal) in ŞNB are partially different from clay samples. The total of trace elements in coal bands is slightly higher than that in clay samples (Σ: 1501 ppm), but some are very high (As: 26 ppm, Cs: 24.73 ppm, Ni: 93 ppm, Sc: 42 ppm, V: 334 ppm, Tl: 93.87 ppm). The REE (except La) values of coal belts are very high compared to clay samples (ΣREE: 310 ppm, ΣLREE: 166 ppm, ΣMREE: 27.1 ppm and ΣHREE: 117 ppm).

Clay formation in ŞNB is the result of different alteration processes. Some researchers have emphasized the formation of Şile kaolin deposits in two stages (Özdamar, 1998; Canberk, 2002; Ece et al., 2003). According to Ece et al. (2003), in the first stage, halloysite-kaolinite formation occurred with the in-situ decomposition of andesitic volcanics (agglomerates, tuff). Our field studies and drilling data revealed an in-situ alteration zone of Mesozoic-aged andesitic rocks at the bottom of some open-quarry within the Neogene sequence. On the other hand, weathering alteration zones of Paleozoic sandstones may also exist in the pre-deposition period. It is possible clay transformation from the feldspars and cement of the sandstones. Finally, another issue is that it is possible to have alteration zones in the granitic pluton geographically close to the ŞNB. For example, likely, the exposition area of the Upper Cretaceous aged Çavuşbaşı granodiorite (Ayanoğlu, 2018) in the near west of ŞNB was much more expansive in the Neogene time. Material may be transported from the granitic rocks to the ŞNB. The second alteration process is the post-deposition period, which results in sedimentary clay formation. The field observations show that the Neogene sequence's clay and coal-rich lower zone was deposited in a shallow lake, lagoon and swamp environment. Ece and Nakagawa (2003) and Ece et al. (2003) explained the kaolinization at this stage. It is possible that the material remained in the water and land environment for short periods. Although they have no lateral continuity in the basin, there are three coals and some organic-rich (clay coal, coal clay) levels. On the other hand, gypsum was only found in the coal levels in the ŞNB. The presence of gypsum and high sulfur content probably indicates bacterial sulfur production. During the geological process, the fragments transported to the basin varied mineralogically and dimensionally, and the physicochemical conditions of the environment probably changed in short intervals. The most distinctive feature of the ŞNB is that it is a Ca-poor sedimentary sequence. This result is evident from the mineralogical and chemical composition of the basin.

The source of the materials deposited in the ŞNB are various rock units of Paleozoic and Mesozoic age around the basin. In other words, it would not be correct to consider the sediment source in the basin as a single geological unit because the clay levels of the basin have variable geochemical character both laterally and vertically. In addition, there are clay and sand levels in the basin that are repetitive on a vertical scale and transitional to each other on a lateral scale. Moreover, the general mineralogical composition of the clay levels in the basin does not exactly resemble that of the surrounding basement rock units. For these reasons, we cannot explain the formation of the current clay and sand levels in the ŞNB by alterations of Paleozoic sandstones, Mesozoic volcanics, or granitic rocks alone. Paleozoic sandstones are rich in mica, but mica is almost absent in the clays of the ŞNB. We can mainly think of the presence of smectite in clay levels in this sense (mica-smectite transformation). The presence of smectite in the basin varies laterally and vertically. While some clay levels contain significant amounts of smectite, others have none. Just as we cannot associate the quartz abundance in the ŞNB with only andesitic volcanics, we cannot associate it with the very fine-grained quartz of Paleozoic sandstones containing high amounts of feldspar. This large volume of quartz sand also suggests the existence of a basement of granitic origin.

## 6. Conclusions

There are no significant vertical and lateral differences in the clay levels of the ŞNB for the major oxides except for $K_2O$, MgO and $Fe_2O_3$. ŞNB is a basin poor in Ca and Na. $K_2O$ in the ŞNB indicates a significant geological basement difference. The clay levels over the Paleozoic sandstones contain $K_2O$ much higher than the clays over the Mesozoic andesite rocks. $Fe_2O_3$ and $Fe_2O_3$ + MgO differ geographically. These values are higher in the eastern part of the basin. Trace elements and REEs in the clay levels of the ŞNB showed differences in lateral and vertical transitions depending on the bedrock group of the basin. 1) REEs are high in the west, northwest, and east of the basin, and low in the center. 2) ΣREE ΣLREE, ΣMREE, ΣHREE, ΣHREE/ΣMREE+ΣLREE, Ce/Ce*, Eu/Eu*, Yb/Yb* and LaN/YbN values in clay layers overlying Paleozoic aged sandstones are higher than those in clays overlying Mesozoic aged andesites. 3) All REE groups of the lower clay levels in the Neogene sequence are higher than those of the upper clays. 4) There are clay levels in the basin that have been exposed to different alteration processes. The lowest clay level in some sections is most likely formed due to in-situ alteration of the Mesozoic andesites. These are probably the uppermost kaolinitic levels of volcanic rocks that should not be included in the Neogene.

On the other hand, the clay levels of ŞNB, which have the composition of kaolinite + illite + Ca-smectite + mixed layered phase (I/S) as clay minerals, have much higher trace element and REE values than the sand levels. This result from the clay minerals' primary material character, ion exchange, and adsorption capabilities. Interpretation of ŞNB from lithostratigraphic, mineralogical and geochemical perspectives, both based on clay levels only and also taking into account sand levels, we reached the following conclusions: 1) Origin of the ŞNB cannot be explained by the influence of a single basement rock group. The material must have come to the basin from Paleozoic sandstones, Mesozoic volcanic rocks, and even granodiorite. 2) The mineral type and size of the material coming into the basin have changed frequently, and, the alteration types and sedimentary environmental conditions of the basin have changed frequently.


## Acknowledgment

The authors are grateful to Adnan Geredeli (Chairman of the Board of Directors; SERHAM, Ceramic Glass and Cement Raw Materials Industrialists Association, Türkiye) for his valuable contributions. The authors are also grateful to Dr. Davut Laçin and two anonymous reviewers for their extremely careful and constructive reviews. They are also grateful to Dr. Halim Mutlu for his insightful editorial comments and suggestions.


## References


Abdüsselamoğlu, Ş. 1963. New stratigraphic and paleontological data in the Paleozoic terrain outcropping to the east of the Bosphorous (İstanbul). Bulletin of the Mineral Research and Exploration 60, 1–7 (in Turkish with English abstract).

Akyüz, H. S. 2010. Paleozoic Sequence of Istanbul and its surroundings. In: Örgün Y, Şahin S (editors). Proocedings of Geology of İstanbul Symposium, İstanbul, 49–62 (in Turkish with English abstract).

Arkun, O. 1985. Istanbul-Şile, Avcıkoru-Karakiraz villages clay-coal-sand fields. In: Gündoğdu MN, Aksoy H (editors). Proceedings of II. National Clay Symposium, Ankara. 405–416 (in Turkish with English abstract).

Ayanoğlu, E. 2018. Age and petrogenesis of the Çavuşbaşı granodiorite. M.Sc. Thesis, İstanbul Technical University, Eurasia Institute of Earth Sciences, İstanbul 59p.

Baykal, F. 1943. Geology of Şile region. İstanbul University, Faculty of Science Monography–3, 81p (in Turkish).

Baykal, F., Kaya, O. 1965. About İstanbul Silurian. Bulletin of the Mineral Research and Exploration 64, 1–8 (in Turkish with English abstract).

Baykal, F., Önalan, M. 1979. Şile sedimentary melange (Sile Olistostrome). In: Proceeding of Altınlı Symposium. Geological Society of Turkey - İstanbul University, Depertment of Geological Enginering, Ankara, 15–25 (in Turkish with English abstract).

Boxleiter, A., Elliott, W. C. 2023. Rare-earth minerals in kaolin ore, mine tailings, and sands-Central Georgia, Upper Coastal Plain. Clays and Clay Minerals 71, 274–308.

Boynton, W. V. 1984. Geochemistry of the rare earth elements: Meteorite studies. In: Henderson P (editor). Rare Earth Element Geochemistry, Elsevier, Amsterdam, 63–114.

Canberk, M. 2002. The Alteration of volcanic rocks in Şile-Sülüklü region, mineralogy of the industrial clays and geochemistry. M.Sc. Thesis, İstanbul Technical University, Institute of Science and Technology, İstanbul, 75p.

Cao, Z., Wang, Q., Cheng, H. 2021. Recent advances in kaolinite-based material for photocatalysts. Chinese Chemical Letters 32, 2617–2628.

Chung, F. H. 1975. Quantitative interpretation of X-ray diffraction patterns of mixtures III; simultaneous determination of a set of reference intensities. Journal of Applied Crystallography 8, 17–19.

Condie, K. C. 1993. Chemical composition and evolution of the Upper Continental Crust, contrasting results from surface samples and shales. Chemical Geology 104, 1–37.

Çelik Karakaya, M., Karakaya, N., Temel, A., Yavuz, F. 2021. Mineralogical and geochemical properties and genesis of kaolin and alunite deposits SE of Aksaray. Applied Geochemistry 124, 104830.

Çiflikli, M. 2020. Hydrothermal alteration-related kaolinite/dickite occurrences in ignimbrites: An example from Miocene ignimbrite units in Avanos, Central Turkey. Arabian Journal of Geosciences 13. 1044–1062.

Çoban, F., Ece, Ö. I., Yavuz, O., Özdamar, Ş. 2002. Petrogenesis of volcanic rocks and clay mineralogy and genesis of underclays, Şile Region, Turkey. Neues Jahrbuch für Mineralogie-Abhandlungen 178, 1–25.

Dill, H. G. 2016. Kaolin: Soil, rock and ore: From the mineral to the magmatic, sedimentary and metamorphic environments. Earth-Science Reviews 161, 16–129.

Ece, Ö. I., Nakagawa, Z. 2003. Alteration of volcanic rocks and genesis of kaolin deposits in Şile Region, Northern Istanbul, Turkey, Part-II. Differential mobility of elements, Clay Minerals 38, 529–550.

Ece, Ö. I., Nakagawa, Z., Schroeder, P. A. 2003. Alteration of volcanic rocks and genesis of kaolin deposits in Şile Region, northern Istanbul, Turkey. Part-I. Clay Mineralogy. Clays and Clay Minerals 51, 675–688.

Ekinci-Şans, B., Esenli, F., Kadir, S., Elliott, W. C. 2015. Genesis of smectite in siliciclastics and pyroclastics of the Eocene İslambeyli Formation in the Lalapaşa region, NW Thrace, Turkey. Clay Minerals 50, 459–483.

Ercan, T. 1979. Cenozoic volcanism in Western Anatolia. Journal of Geological Engineering 9, 23–46. (in Turkish with English abstract).

Erdoğan, M., Esenli, F., Öztaş, T., Kariptaş, Ç., Yüksekol, Ö.Y., Fitoz, E., Talay, T., Bostancıoğlu, İ. 2023. Current and potential status of clay and sand raw material of İstanbul. Proocedings of Geology of İstanbul Symposium-6, İstanbul, 197–202 (in Turkish with English abstract).

Esenli, F., Ekinci Şans, B. 2023. Clay mineralogy of İstanbul Tertiary units. Proocedings of Geology of İstanbul Symposium-6, İstanbul, 203–209 (in Turkish with English abstract).

Esenli, F., Özdamar, Ş., Tunçdemir, H., Ekinci Şans, B., Sarıkaya, O., Kumral, M. 2024. Lithostratigraphy, mineralogy, geochemistry and raw material reserves of the Şile clay-sand-coal basin. Madencilik Türkiye 117, 88–92 (in Turkish).

Gedik, İ., Pehlivan, Ş., Timur, E., Duru, M., Altun, İ., Akbaş, B., Özcan, İ., Alan, İ. 2005. Geology of Kocaeli Peninsula. General Directorate of Mineral Research and Exploration, Report Nr: 10774, Ankara (in Turkish).

Genç, C. 2019. Revealing the economic importance of Şile Region clay and sands, especially in terms of the ceramics industry and other related sectors. Ceramics Research Center, Anadolu University, Report, 54s (in Turkish).

Gianni, E., Avgoustakis, K., Papoulis, D. 2020. Kaolinite group minerals: Applications in cancer diagnosis and treatment. European Journal of Pharmaceutics and Biopharmaceutics 154, 359–376.

Güngör, N., Gökçen Demir, B., Kaçmaz, E. 2015. The indispensable importance of the Istanbul-Şile Neogene Basin and its contributions to the economy. Madencilik Türkiye 45, 88–93 (in Turkish).

Huggett, J. M. 2005. Sedımentary rocks/clays and their diagenesis. Encyclopedia of Geology 62–70.

Kadir, S., Ateş, H., Erkoyun, H., Külah, T., Esenli, F. 2022. Genesis of alunite-bearing kaolin deposit in Mudamköy member of the Miocene Göbel Formation, Mustafakemalpaşa (Bursa), Turkey. Applied Clay Science 221, 106407.

Kaya, O. 1973. Paleozoic of İstanbul. Ege University, Faculty of Science Publication 40, 1–25 (in Turkish).

Keskin, M., Ustaömer, T., Yeniyol, M. 2003. Stratigraphy, petrology and tectonic setting of Upper Cretaceous volcano-sedimentary units, north of İstanbul, Turkey. In: Güngör Y (editor). Proocedings of Geology of İstanbul Symposium, İstanbul, 23–35 (in Turkish with English abstract).

Koç, Ş., Baştuğ, A. Y., Çelik, H. 2014. Investigation of quartz sand and assessment of economic importance around İstanbul-Şile. Ankara University Scientific Research Project (Nr: 12Ö4343009), Ankara, 32p (in Turkish).

Laçin, D., Aysal, N., Öngen, S. 2021. Geological, mineralogical and technological properties of Oligocene-Miocene clay deposits in altered volcanic rocks for the ceramic industry (Western Anatolia, Turkey). Arabian Journal of Geosciences 14, 1904.

MTA, 2017. 1:250,000 Scale Geological Map of Turkey. General Directorate of Mineral Research and Exploration, Ankara, Turkey.

Murray, H. H., Keller, W. D. 1993. Kaolins, kaolins, kaolins. In: Murray HH, Bundy WM, Harvey CC (editors). Kaolin Genesis and Utilization. Special Publication 1, The Clay Minerals Society, Boulder, CO, 1–24.

Norouzi, M., Abedini, A., Calagari, A. A., Kangarani Farahani, F. 2021. Geochemistry of kaolin occurrence in the Abolhasani-Zereshkouh area, southeast of Damghan, NE Iran. Scientific Quarterly Journal of Geosciences 30(118), 123–134.

Okay, A. I., Kylander-Clark, A. R. C. 2023. No sediment transport across the Tethys Ocean during the latest Cretaceous: detrital zircon record from the Pontides and the Anatolide–Tauride Block. International Journal of Earth Sciences 112, 999–1022.

Okay, A. I., Şengör, A. M. C., Görür, N. 1994. Kinematic history of the history of the Black Sea and its effect on the surrounding regions. Geology 22, 267–270.

Omang, B. O., Kudamnya, E. A., Owolabi, A. O., Odey, J., Aniwetalu, E. U., Ako, T. A. 2019. Characterization of kaolin deposits in Okpella and Environs, Southern Nigeria. International Journal of Geosciences 10(3), 317–327.

Ömeroğlu Sayıt, I., Günal Türkmenoğlu, A., Sayın, Ş. A., Demirci, C. 2018. Hydrothermal alteration products in the vicinity of the Ahırözü kaolin deposits, Mihalıççık-Eskişehir, Turkey. Clay Minerals 53, 289–303.

Özdamar, Ş. 1998. Clay mineralogy of underclays in the Sile region. M.Sc. Thesis, İstanbul Technical University, Institute of Science and Technology, İstanbul, 117p.

Özdamar, Ş., Ece, Ö. I., Kayacı, K., Küçüker, A. S. 2007. Mineralogical and technological properties of underclays in Şile region, İstanbul, Turkey. Industrial Ceramics 27(3), 1–11.

Özgül, N. 2011. Geology of Istanbul Province Area. General geological characteristics of the Istanbul provincial area. Istanbul Metropolitan Municipality, Planning and Zoning Department, Soil and Earthquake Investigation Directorate. İstanbul, 305p (in Turkish).

Özşahin, E., Ekinci, D. 2013. Main lines of the geomorphological features of İstanbul's Anatolian side. Journal of Geography 27, 14–37 (in Turkish with English abstract).

Prasad, M. S., Reid, K. J., Murray, H. H. 1991. Kaolin: processing, properties and applications. Applied Clay Science 6(2), 87–119.

Sekmen, T. 2019. Geomorphology, change and development of coastal region between Anatolian Feneri-Ağva. M.Sc. Thesis, Istanbul University, Institute of Social Sciences, Department of Geography, İstanbul, 215p.

Senkayi, A. L., Dixon, J. B., Hossner, L. R., Abder-Ruhman, M., Fanning, D. S. 1984. Mineralogy and genetic relationships of tonstein, bentonite and lignitic strata in the Eocene Yegua Formation of East-Central Texas. Clays and Clay Minerals 32, 259–271.

Sipahi, H., Kuzum, Ç. 2011. Stratigraphic features of the Şile Neogene sequence. Madencilik Türkiye, 17, 66–71 (in Turkish).

Spears, D. A., Kanaris-Sotiriou, R. 1979. A geochemical and mineralogical investigation of some British and other European tonstein. Sedimentology 26, 407–425.

Şengör, A. M. C., Yılmaz, Y. 1981. Tethyan evolution of Turkey: a plate tectonic approach. Tectonophysics 75, 181–241.

Taylor, S. R., McLennan, S. M. 1995. The geochemical evolution of the continental crust. Reviews in Geophysics, 33, 241–265.

Tüysüz, O. 1999. Geology of the Cretaceous sedimentary basins of the Western Pontides. Geological Journal 34, 75–93.

Ünal Ercan, H., Ece, Ö. I., Çiftçi, E., Aydın, A. 2022. Comparison of epithermal kaolin deposits from the Etili Area (Çanakkale, Turkey): Mineralogical, geochemical, and isotopic characteristics. Clays Clay Minerals 70, 753–779.

Whitney, D. L., Evans, B. W. 2010. Abbreviations for names of rock-forming minerals. American Mineralogist 95, 185–187.

Yanık, G., Ceylantekin, R., Taşçı, E. 2018. The Gümüşköy (Kütahya/Turkey) kaolin deposit and its ceramic properties. Clay Minerals 53 (3), 515–524.

Yeniyol, M. 1984. Occurrence of clays of İstanbul. Geological Bulletin of Türkiye 5, 143–150 (in Turkish with English abstract).

Yeniyol, M., Ercan, T. 1989. Geology of the Northern İstanbul, petrochemical characteristics of Upper Cretaceous volcanism and its regional distribution in Pontides. İstanbul Earth Sciences Review 7, 125–147 (in Turkish with English abstract).

Yılmaz, Y., Tüysüz, O., Yiğitbaş, E. 1997. Geology and tectonic evolution of the Pontides. Regional and Petroleum Geology of the Black Sea and Surrounding Region, AAPG Memoir- 68, 183–226.

Zhoui Y., Ren, Y., Bohor, B.F. 1982. Origin and distribution of tonsteins in lake Permien coal seams of southwestern China. International Journal of Coal Geology 2, 49–77.

Zotov, A., Mukhamet-Galeev, A., Schott, J. 1998. An experimental study of kaolinite and dickite relative stability at 150–300 8C and the thermodynamic properties of dickite. American Mineralogist 83, 516–524.